

# Metal $\pi$ Complexes of Carbazole Derivatives for Optoelectronics: Synthesis, Structures, and UV–Visible Absorption Spectra of (3-Amino-9-ethylcarbazole)chromium Tricarbonyl Complexes

Kanyi Shen,<sup>†,‡</sup> Xiaohui Tian,<sup>\*,†,‡</sup> Juhua Zhong,<sup>§</sup> Jiaping Lin,<sup>†</sup> Yi Shen,<sup>‡</sup> and Peiyi Wu<sup>\*,‡</sup>

School of Materials Science and Engineering, East China University of Science and Technology, Shanghai 200237, China, The Key Laboratory of Molecular Engineering of Polymers (Fudan University), Ministry of Education, Shanghai 200433, China, and Department of Physics, East China University of Science and Technology, Shanghai 200237, China

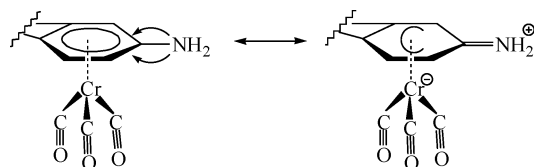
Received June 18, 2004

Chromium tricarbonyl complexes  $\eta^6$ -bonded to 3-amino-9-ethylcarbazole at either the  $\text{NH}_2$ -substituted aryl ring (**1**) or the unsubstituted aryl ring (**2**) have been synthesized and their UV–visible absorption spectra determined. In comparison to **2**, **1** causes a subtle blue shift in the metal-to-ligand charge-transfer band along with spectral shape changes due to electron transfer from the  $\text{NH}_2$  substituent to the  $\text{Cr}(\text{CO})_3$  center.

## Introduction

Carbazole and its derivatives are of interest as electron donor and hole transport materials capable of sensitizing photoconductivity by the addition of an amount of electron acceptor.<sup>1,2</sup> Some publications have demonstrated that incorporation of electron-accepting groups into carbazole-containing polymers enhances their photoconductivity to a greater extent than just a simple blending of small molecules thereto.<sup>3</sup> These facts have aroused our interest in the complexes of carbazole-containing organics with an acceptor metal moiety such as a  $\text{Cr}(\text{CO})_3$  group, which exhibits a strong electron-withdrawing effect, comparable to that of a nitro substituent on an aryl ligand.<sup>4</sup> Logically, this idea could be extrapolated to a useful push–pull molecular structure in a metal–organic environment to generate optoelectronic functional compounds.<sup>5</sup> In addition to the donor-substitution effect on the carbazole moiety, the

properties of this push–pull molecular structure may also be dependent upon both the nature of the substituent and its relative position with respect to the  $\text{Cr}(\text{CO})_3$  fragment.<sup>6</sup> For example, coordinating  $\text{Cr}(\text{CO})_3$  to 3-amino-9-ethylcarbazole (AECz) may provide structural/electronic diversity that leads to interesting optical properties. Thus, a  $\pi$ -donating  $\text{NH}_2$  substituent would be expected to increase the electron transfer to  $\text{Cr}(\text{CO})_3$ , and this can be represented, in valence bond terms, as an increased contribution from a zwitterionic resonance form having a negative charge localized on chromium and a positive charge on the  $\text{NH}_2$  substituent, i.e.<sup>7</sup>



In this contribution, we wish to present the synthesis, structures, and coordination position–photophysical

\* To whom correspondence should be addressed. E-mail: tianxh@263.net (X.T.); peiyiwu@fudan.edu.cn (P.W.)

<sup>†</sup> School of Materials Science and Engineering, East China University of Science and Technology.

<sup>‡</sup> The Key Laboratory of Molecular Engineering of Polymers (Fudan University).

<sup>§</sup> Department of Physics, East China University of Science and Technology.

(1) (a) Borsenberger, P. M.; Weiss, D. S. *Organic Photoreceptors for Imaging Systems*; Marcel Dekker: New York, 1993. (b) Hu, B.; Yang, Z.; Karasz, F. E. *J. Appl. Phys.* **1994**, *76*, 2419–2422. (c) Gebler, D. D.; Wang, Y. Z.; Fu, D.-K.; Swager, T. M.; Epstein, A. J. *J. Chem. Phys.* **1998**, *108*, 7842–7848.

(2) Mylnikov, V. S. *Adv. Polym. Sci.* **1994**, *115*, 1–88.

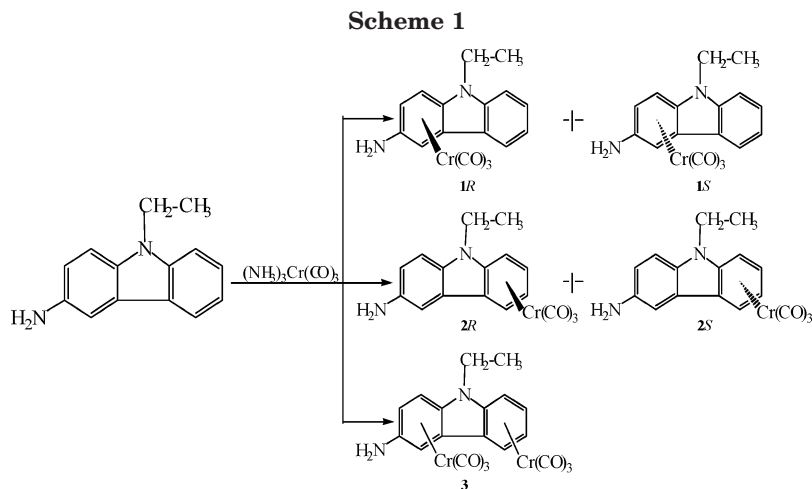
(3) (a) Chang, D. M.; Gromelski, S.; Rupp, R.; Mulvaney, E. J. *J. Polym. Sci., Polym. Chem. Ed.* **1977**, *15*, 571–584. (b) Mulvaney, J. E.; Brand, R. A. *Macromolecules* **1980**, *13*, 244–248. (c) Jenekhe, S. A.; Lu, L.; Alam, M. M. *Macromolecules* **2001**, *34*, 7315–7324.

(4) Nicholls, B.; Whitting, M. C. *J. Chem. Soc.* **1959**, 551.

(5) (a) Kanis, D. R.; Ratner, M. A.; Marks, T. J. *J. Am. Chem. Soc.* **1992**, *114*, 10338–10357. (b) Muetterties, E. L.; Bleeke, J. R.; Wucherer, E. J.; Albright, T. A. *Chem. Rev.* **1982**, *82*, 499–525. (c) Gilbert, T. M.; Hadley, F. J.; Bauer, C. B.; Rogers, R. D. *Organometallics* **1994**, *13*, 2024–2034.

(6) (a) Howell, J. O.; Goncalves, J. M.; Amatore, C.; Klasing, L.; Wightman, R. M.; Kochi, J. K. *J. Am. Chem. Soc.* **1984**, *106*, 3968–3976. (b) Albright, T. A.; Hofmann, P.; Hoffmann, R. *J. Am. Chem. Soc.* **1977**, *99*, 7546–7557. (c) Chinn, J. W.; Hall, M. B. *J. Am. Chem. Soc.* **1983**, *105*, 4930–4941. (d) Semmelhack, M. F.; Garcia, J. L.; Cortes, D.; Farina, R.; Hong, R.; Carpenter, B. K. *Organometallics* **1983**, *2*, 467–469. (e) Solladie-Cavallo, A.; Wipff, G. *Tetrahedron Lett.* **1980**, 3047–3050. (f) Dillow, G. W.; Kebarle, P. *J. Am. Chem. Soc.* **1989**, *111*, 5592–5596. (g) Chowdhury, S.; Kishi, H.; Dillow, G. W.; Kebarle, P. *Can. J. Chem.* **1989**, *67*, 603–610. (h) Gould, I. R.; Ege, D.; Moser, J. E.; Farid, S. *J. Am. Chem. Soc.* **1990**, *112*, 4290–4301. (i) Neikam, W. C.; Desmond, M. M. *J. Am. Chem. Soc.* **1964**, *86*, 4811–4814. (j) Miller, L. L.; Nordblom, G. D.; Mayeda, E. A. *J. Org. Chem.* **1972**, *37*, 916–918. (k) Turner, D. W. *Adv. Phys. Org. Chem.* **1966**, *4*, 31–71.

(7) (a) Hunter, A. D.; Shilliday, L.; Furey, W. S.; Zaworotko, M. J. *Organometallics* **1992**, *11*, 1550–1560. (b) Hunter, A. D.; Mozol, V.; Tsai, S. D. *Organometallics* **1992**, *11*, 2251–2262. (c) Li, J.; Hunter, A. D.; McDonald, R.; Santarsiero, B. D.; Bott, S. G.; Atwood, J. L. *Organometallics* **1992**, *11*, 3050–3055.



property relationship of (3-amino-9-ethylcarbazole)chromium tricarbonyl complexes. It is noteworthy that the  $\text{Cr}(\text{CO})_3$  coordination to the unsubstituted aryl ring (**2**) is thermodynamically more stable than that to the  $\text{NH}_2$ -substituted aryl ring (**1**).

### Results and Discussion

Reaction of AECz with  $(\text{NH}_3)_3\text{Cr}(\text{CO})_3$  in dioxane proceeded with a simultaneous color change from yellow to dark red. Removal of the solvent and one crystallization of the residue from  $\text{CH}_2\text{Cl}_2$ /hexane afforded a mixture of mono- and bis(chromium tricarbonyl) complexes, as depicted in Scheme 1, in which **1** (*R* and *S*) predominated and **2** (*R* and *S*) was present in a relatively low yield of  $\leq 10\%$ , together with a minor bis(chromium tricarbonyl) complex of AECz, **3**.<sup>8</sup> **1** and **2** were separated by chromatography and obtained as reddish orange crystals which are quite stable in the solid state. However, an attempt to purify **3** to an analytically pure form failed, due to its limited yield and extreme sensitivity toward air and sunlight in solution. The coordination sites of the carbazole at either the  $\text{NH}_2$ -substituted aryl ring or the unsubstituted aryl ring are deduced from the typical high-field coordination shifts in  $^1\text{H}$  and  $^{13}\text{C}$  NMR spectra. These two complexes are soluble in common organic solvents except alkanes, in which they have low solubility and can be crystallized therefrom. Under an inert atmosphere, a solution of **2** is stable at room temperature for several days, whereas solutions of **1** can only be stored for a short period of time even with sheltering from sunlight. In appropriate solvents, **1** could partially be converted into **2** at ambient temperature. Diethyl ether, THF, and pyridine are found to be good solvents for such conversion, probably due to their ability to induce the decomplexation of **1**, generating the labile intermediate  $(\text{solvent})_3\text{Cr}(\text{CO})_3$ , which further affords "hot"  $\text{Cr}(\text{CO})_3$  particles and randomly attacks aryl rings of the carbazole moiety.<sup>9</sup> In contrast, conversion from **2** to **1** failed under the same conditions because of its surprising stability to these

solvents. Kinetic curves for the conversion of **1** into **2** in diethyl ether at 293 K are shown in Figure 1. An

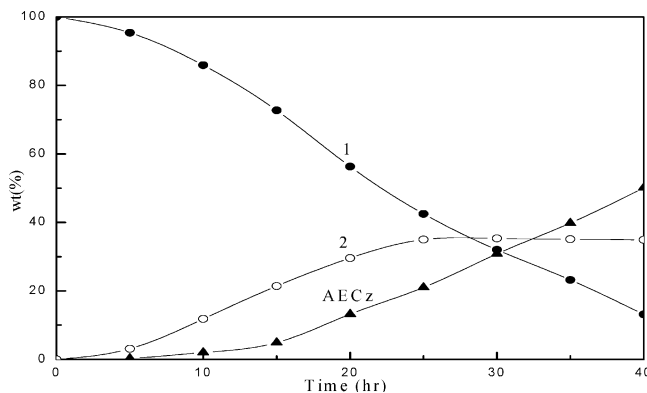


**Figure 1.** Kinetic curves of conversion of **1** into **2** in diethyl ether at 293 K.

accumulation of AECz in the system increases with an increasing amount of **2**, indicating that this conversion proceeds through the process of  $\mathbf{1} \rightarrow \text{AECz} \rightarrow \mathbf{2}$ . Accordingly, **1** represents the kinetically controlled product and **2** the thermodynamically controlled one.

The structures of **1** and **2** have been determined by X-ray crystallography, as shown in Figure 2. **1** and **2** are isomorphous chiral molecules exhibiting the expected three-legged piano-stool structures; in each case, both *R* and *S* enantiomers cocrystallize in the centrosymmetric achiral  $P2_1/n$  space group.<sup>10</sup> As discussed previously by Hunter et al., the  $\pi$ -donating substituents will cause the coordinated aryl ring to bend away from the metal.<sup>7</sup> Such a bend clearly occurs in **1**, and the observed magnitude of this structural distortion appears to be dependent primarily upon the magnitude of  $\pi$ -donor ability of the substituent. Thus, the very strongly  $\pi$ -donating  $\text{NH}_2$  substituent shows a similarly large distortion from planarity with its ipso carbon, C4 (0.0607 Å), being bent strongly away from the Cr atom, while the more weakly  $\pi$ -donating  $\text{NEtAr}$  substituent (the N1 atom in **1** cannot  $\pi$  interact with the coordinated aryl ring as effectively as the N2 atom because it is also

(8) Mass spectra of the mixture are all simple and in agreement with their compositions. The molecular ion  $[\text{M}^+]$  and other main fragments, such as  $[\text{M} - n\text{CO}]$  ( $n = 1-3$ ), are observed for **1** and **2**. Additionally, the molecular ion  $[\text{M}^+]$  and fragments  $[\text{M} - n\text{CO}]$  ( $n = 1-6$ ) for **3** are also observed.

(9) Oprunenko, Y.; Malyugina, S.; Nesterenko, P.; Mityuk, D.; Malyshev, O. *J. Organomet. Chem.* **2000**, 597, 42-47.

(10) Both *R* and *S* enantiomers, in which the chromium atom is respectively attached to the opposite side of the same aryl ring, are present in a 1:1 ratio in the crystals and have been confirmed by crystallographic rather than spectroscopic techniques (see the Supporting Information).

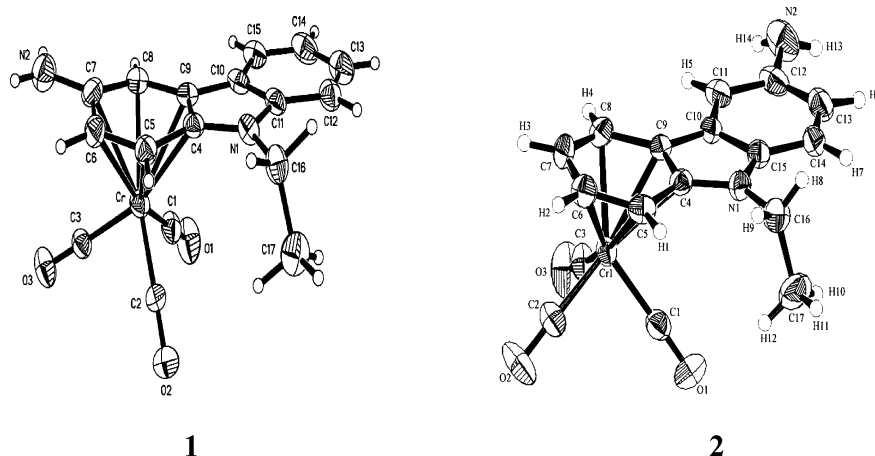


**Figure 2.** ORTEP drawings of **1** (left) and **2** (right) with thermal ellipsoids at the 30% probability level.

$\pi$  bonded to the other uncoordinated aryl ring) shows a somewhat smaller structural distortion with its attached  $\eta^6$ -aryl carbon C7 (0.0587 Å), in the same direction. In the case of **2**, the coordinated ring is virtually planar with the carbon attached to the donor N(Et)Ar group, C4, at a maximum deviation of 0.0492 Å away from the Cr atom, while C5 deviates 0.0518 Å toward the Cr atom. All carbon–carbon distances in the coordinated rings are routinely longer than those in the corresponding uncoordinated rings. This likely reflects a slight loss in aromaticity upon coordination, owing to back-donation of electron density from the metal into the  $\pi^*$  orbitals of the ring. The pronounced difference among bond distances for the carbons bound to N1 (i.e. C4–N1 = 1.370 Å, C11–N1 = 1.390 Å, and C16–N1 = 1.448 Å) in **1** illustrates that the electron density is dominantly localized on the coordinated ring rather than spread out over the entire carbazole moiety. Similarly, the rather wide range of N1 bond distances (i.e. C4–N1 = 1.368 Å, C15–N1 = 1.395 Å, and C16–N1 = 1.464 Å) in **2** emphasizes the relatively high localization on the coordinated ring without an NH<sub>2</sub> substituent. Contribution of the  $\pi$ -donating NH<sub>2</sub> substituent to its attached coordinated ring can be further illustrated by the junction carbon distances, which appear to be 1.402/1.434 Å in the uncoordinated/coordinated cases of the unsubstituted aryl ring and 1.404/1.412 Å for the substituted aryl ring. An upfield shift of NH<sub>2</sub> in the <sup>1</sup>H NMR of **1** (3.70 ppm) relative to **2** (5.41 ppm) provides additional data for this point. It also reveals a change in nitrogen's hybridization from sp<sup>3</sup> toward sp<sup>2</sup>, leading to a flattening of the pyramidal aryl–NH<sub>2</sub> group and a shortening of its bond distance from 1.392 to 1.372 Å.

Another important difference between **1** and **2** is the orientation of the carbonyl groups with respect to the substituents on the coordinated ring. According to Gilbert et al., this orientational preference is electronically controlled only when the substituent is highly electron-donating; otherwise, other factors such as crystal-packing forces can take precedence.<sup>11</sup> The conformation of the Cr(CO)<sub>3</sub> fragment in **1** is found to be intermediate between staggered and eclipsed with car-

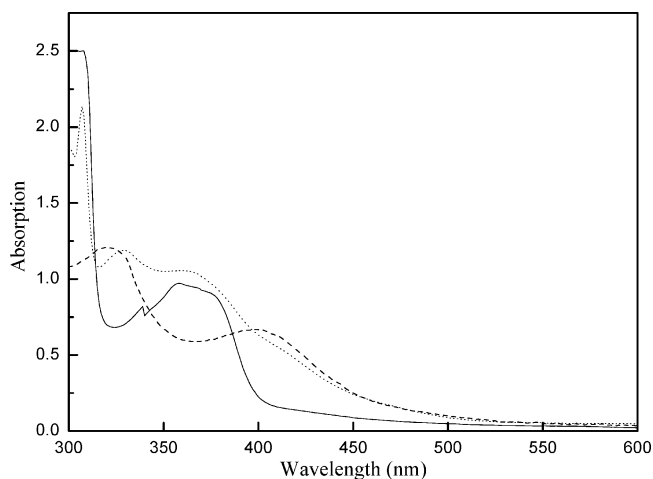


**Figure 3.** UV–vis absorption spectra of **1** (---), **2** (···), and AECz (—) in dichloromethane at 298 K.

bonyl groups being located near C5, C7, and C9, representing the best compromise between the electron-donor demands of the NH<sub>2</sub> and the N(Et)Ar substituents. However, **2** has a tendency to adopt a N(Et)Ar group-eclipsed conformation with the torsion angle of C4–cent–Cr–C1 approximately equal to 0°. As a result of the steric congestion for crystal packing of the three-dimensional molecules, the methyl group lies on the same side of the metal center and is nearly perpendicular to the carbazole plane with 95.0° in **1** and 99.2° in **2**, respectively. The carbazole ring and its attached N-methene carbon are nearly coplanar, although a slight boat-type deformation displays that both of the aryl rings lie away from the approximate plane defined by the central heterocycle with a dihedral angle of 7.28° for **1** and 7.31° for **2**, respectively.

The UV–visible absorption spectra of **1** and **2** in dichloromethane are shown in Figure 3, and the data are summarized in Table 1. In accordance with the perpendicular orientation of the transition dipole moment to the molecular main dipole axis, the metal-to-ligand charge-transfer (MLCT) transition band is expected to be smaller in its intensity.<sup>5a,12</sup> We tentatively assign the lower energy band at ca. 405–415 nm to an

(11) (a) Gilbert, T. M.; Hadley, F. J.; Simmons, M. D.; Bauer, C. B.; Rogers, R. D. *J. Organomet. Chem.* **1996**, *510*, 83–92. (b) Gilbert, T. M.; Bond, A. H.; Rogers, R. D. *J. Organomet. Chem.* **1994**, *479*, 73–86.

(12) Because a substantial electron density transfers from a “non-bonding” metal-based state to a ligand-based  $\pi^*$  state, the energy of the MLCT band is expected to be at an energy lower than that of the predominant  $\pi$  to  $\pi^*$  transition in the free ligand.

**Table 1. UV–Visible Absorption Spectral Data for 1, 2, and AECz at 298 K**

compd	$\lambda_{\text{max}}/\text{nm}$ ( $\epsilon/\text{dm}^3 \text{ mol}^{-1} \text{ cm}^{-1}$ )
AECz	355 (24 500), 380 (sh, 21 250)
<b>1</b> <sup>a</sup>	320 (37 500), 405 (20 300)
<b>1</b> <sup>b</sup>	325 (34 500), 410 (16 800)
<b>2</b> <sup>a</sup>	330 (25 200), 365 (22 050), 415 (sh, 10 500)
<b>2</b> <sup>b</sup>	335 (24 300), 370 (21 300), 420 (sh, 10 100)

<sup>a</sup> Measured in dichloromethane. <sup>b</sup> Measured in C<sub>6</sub>F<sub>6</sub>.

MLCT transition. In view of the fairly large extinction coefficient ( $10^4 \text{ dm}^3 \text{ mol}^{-1} \text{ cm}^{-1}$ ), which is an order of magnitude larger than that ( $10^3 \text{ dm}^3 \text{ mol}^{-1} \text{ cm}^{-1}$ ) commonly observed for (arene)chromium tricarbonyl complex MLCT transitions,<sup>5c,13</sup> as well as the fact that the free ligand per se has an absorption tail extending far into the visible region, it is likely that this transition may contain considerable ligand field character. The strong absorption band of **2** at 365 nm, which also occurs in the free ligand, is assigned to the ligand-localized  $\pi-\pi^*$  transition from the NH<sub>2</sub>-substituted aryl ring. **1** does not show such an absorption in the same spectral region, presumably due to a significant perturbation induced by Cr(CO)<sub>3</sub> coordination. The higher energy absorption bands at ca. 320–330 nm can be regarded as the intraligand  $\pi-\pi^*$  transition (ILCT) on the basis of their higher extinction coefficients. In comparison to **2**, **1** causes a synchronous blue shift of the MLCT and ILCT bands by 10 nm. A similar solvent effect on the MLCT band was also observed in C<sub>6</sub>F<sub>6</sub>, a molecule with low coordination ability (Table 1).<sup>9</sup> The susceptibility of the solution absorption spectra toward the NH<sub>2</sub> substituent–metal architectures would assist us in evaluating the question of how well “matched” the electronic demand of the Cr(CO)<sub>3</sub> center was to that of the coordinated ring.<sup>14</sup> It seems likely that **1**, where the NH<sub>2</sub>-substituted aryl ring is coordinated to the acceptor metal moiety, would prove to be less matched, as indicated by its higher absorption energy of bands relative to **2**, where the acceptor chromium fragment coordinates the unsubstituted aryl ring. This is in agreement with the above-mentioned fact that **1** is unstable in solution and undergoes a conversion of **1** into **2**.

## Conclusions

Synthesis and characterization of (3-amino-9-ethylcarbazole)chromium tricarbonyl complexes have been accomplished. Altering the coordination site from the NH<sub>2</sub>-substituted aryl ring to the unsubstituted one or vice versa causes a redistribution of the charge-transfer electron density, inducing the changes of the geometrical as well as spectral features. Future work will be focused

(13) (a) Kirss, R. U.; Treichel, P. M.; Haller, K. J. *Organometallics* **1987**, *6*, 242–249. (b) Kobayashi, H.; Kobayashi, M.; Kaizu, Y. *Bull. Chem. Soc. Jpn.* **1973**, *46*, 3109–3116. (c) Kobayashi, H.; Kobayashi, M.; Kaizu, Y. *Bull. Chem. Soc. Jpn.* **1975**, *48*, 1222–1227.

(14) A semiempirical molecular orbital calculation predicts that the resulting charge transfer occurs from the coordinated aryl ring to carbonyl groups, although a small charge transfer from the carbonyl ligands back to the coordinated aryl ring may also occur. In fact, the way to divide the charge transfer electron density into the carbonyl and aryl ligands appears to be dependent primarily upon the magnitude of the  $\pi$ -donor or  $\pi$ -acceptor abilities of the substituents on the coordinated aryl ring.

on the optoelectronic behavior of chromium tricarbonyl complexes  $\eta^6$ -bonded to carbazole derivatives.

## Experimental Section

Unless otherwise noted, all manipulations were performed under an atmosphere of dry argon using standard Schlenk and vacuum techniques. Solvents were dried using conventional procedures, distilled under argon, and degassed prior to use. Cr(CO)<sub>6</sub> (99%, Strem Chemistry) was sublimed prior to use. AECz (90%, Aldrich) was used as received. Elemental analyses were carried out on an Elemental Vario EL III analyzer (C, H, N) and TJARIS 1000 instrument (Cr), respectively. Electron-impact mass spectra were recorded on a Micromass GCT (EI, 70 eV) mass spectrometer. <sup>1</sup>H NMR (500 MHz) and <sup>13</sup>C NMR (125 MHz) spectra were recorded on a Bruker AVANCE 500 MHz spectrometer, using CDCl<sub>3</sub> as solvent at 298 K and Me<sub>4</sub>-Si as an internal standard. IR spectra were recorded on a Nicolet Magna-IR 550 instrument in KBr pellets. Column chromatography was performed on Matrix silica 60 (30–70  $\mu\text{m}$ ). UV–vis spectra were obtained on a Varian Cary 500 spectrophotometer rebuilt by OLIS to incorporate computer control. Melting points were measured using a Reichert Thermopan melting point microscope and are uncorrected.

**(3-Amino-9-ethylcarbazole)chromium Tricarbonyl Complexes 1 and 2.** Cr(CO)<sub>6</sub> was reacted to give (NH<sub>3</sub>)<sub>3</sub>Cr(CO)<sub>3</sub> according to a literature method.<sup>15</sup> A mixture of 4.9 g (26.2 mmol) of (NH<sub>3</sub>)<sub>3</sub>Cr(CO)<sub>3</sub> and 3.0 g (14.2 mmol) of AECz was heated under reflux in 100 mL of dioxane for 6 h. After being cooled, the solution was filtered through a Celite filter and the residue was washed with CH<sub>2</sub>Cl<sub>2</sub> (2  $\times$  5 mL). The residue was chromatographed on a 5  $\times$  35 cm silica gel column using ether–THF as eluent. The first zone was eluted with ether/THF (1:1 v/v), and the second zone was eluted with THF. The products were recrystallized three times from CH<sub>2</sub>Cl<sub>2</sub>/*n*-hexane, respectively, to obtain two kinds of reddish orange crystals.

**Complex 1:** yield 3.9 g (49%). Mp: 163–165 °C. Anal. Calcd for C<sub>17</sub>H<sub>14</sub>N<sub>2</sub>O<sub>3</sub>Cr: C, 58.91; H, 4.04; N, 8.09; Cr, 15.03. Found: C, 59.12; H, 4.15; N, 7.98; Cr, 14.89. IR ( $\nu$ (CO); KBr): 1808 (s), 1880 (s), 1949 (s) cm<sup>-1</sup>. <sup>1</sup>H NMR (ppm, numbering from Figure 2): 7.99 (d, 1H, *J* = 7.2 Hz, 7-H), 7.48 (t, 2H, 5,6-H), 7.20 (d, 1H, 4-H), 6.76 (d, 1H, *J* = 6.9 Hz, 1-H), 6.21 (s, 1H, 3-H), 5.30 (d, 1H, *J* = 6.3 Hz, 2-H), 5.47 (s, 2H, 13, 14-H). <sup>13</sup>C NMR (ppm, numbering from Figure 2): 72.0, 76.4, and 77.4 (C5, C8, and C9); 95.1, 109.4, and 114.0 (C6, C7, and C4); 120.2, 120.8, and 122.9 (C12, C14, and C15); 123.3, 134.4, and 142.9 (C10, C13, and C11); 236.3 (C=O). MS (EI, 70 eV; *m/z* (%)): 346.0 (6.51) [M<sup>+</sup>], 318.0 (0.17) [M<sup>+</sup> – CO], 290.0 (8.91) [M<sup>+</sup> – 2CO], 262.0 (56.36) [M<sup>+</sup> – 3CO], 210.0 (82.61) [M<sup>+</sup> – Cr(CO)<sub>3</sub>], 195.0 (100.00), 52 (7.97) [Cr<sup>+</sup>].

**Complex 2:** yield 0.6 g (7.7%). Mp: 156–158 °C. Anal. Calcd for C<sub>17</sub>H<sub>14</sub>N<sub>2</sub>O<sub>3</sub>Cr: C, 58.91; H, 4.04; N, 8.09; Cr, 15.03. Found: C, 59.14; H, 4.09; N, 8.12; Cr, 14.90. IR ( $\nu$ (CO); KBr): 1830 (s), 1850 (s), 1930 (s) cm<sup>-1</sup>. <sup>1</sup>H NMR (ppm, numbering from Figure 2): 7.21 (d, 1H, *J* = 2.1 Hz, 7-H); 7.13 (d, 1H, *J* = 8.6 Hz, 5-H); 6.91 (d, 1H, *J* = 8.6 Hz, 6-H); 6.55 (d, 1H, *J* = 6.4 Hz, 4-H); 5.84 (d, 1H, *J* = 6.9 Hz, 1-H); 5.61 (t, 1H, *J*<sub>1</sub> = 6.6 Hz, *J*<sub>2</sub> = 6.4 Hz, 2-H); 5.06 (t, 1H, *J*<sub>1</sub> = 6.2 Hz, *J*<sub>2</sub> = 6.2 Hz, 3-H); 3.70 (s, 2H, 13, 14-H). <sup>13</sup>C NMR (ppm, numbering from Figure 2): 74.1, 84.5, and 89.1 (C5, C7, and C8); 91.3, 93.0, and 105.7 (C9, C6, and C4); 110.1, 116.8, and 123.3 (C14, C11, and C10); 124.2, 136.0, and 140.9 (C13, C12, and C15); 234.3 (C=O). MS (EI, 70 eV; *m/z* (%)): 346.0 (2.14) [M<sup>+</sup>], 318.0 (1.20) [M<sup>+</sup> – CO], 290.0 (2.77) [M<sup>+</sup> – 2CO], 262.1 (15.55) [M<sup>+</sup> – 3CO], 210.1 (85.39) [M<sup>+</sup> – Cr(CO)<sub>3</sub>], 195.1 (100.00), 51.9 (2.99) [Cr].

(15) Razuvaev, G. A.; Artemov, A. N.; Aladjin, A. A.; Sirotkin, N. I. *J. Organomet. Chem.* **1976**, *111*, 131.

**Table 2. Crystal and Structure Determination Data**

	<b>1</b>	<b>2</b>
empirical formula	C <sub>17</sub> H <sub>14</sub> N <sub>2</sub> O <sub>3</sub> Cr	C <sub>17</sub> H <sub>14</sub> N <sub>2</sub> O <sub>3</sub> Cr
formula wt	346.30	346.30
radiation; $\lambda$ (Å)	Mo K $\alpha$ ; 0.710 73	Mo K $\alpha$ ; 0.710 69
temp (K)	293(2)	298(1)
cryst syst	monoclinic	monoclinic
space group	<i>P</i> 2 <sub>1</sub> / <i>n</i>	<i>P</i> 2 <sub>1</sub> / <i>n</i>
<i>a</i> (Å)	8.4209(8)	12.175(3)
<i>b</i> (Å)	12.8580(12)	13.950(3)
<i>c</i> (Å)	13.9489(13)	10.056(3)
$\alpha$ (deg)	90	90
$\beta$ (deg)	91.840(2)	111.98(2)
$\gamma$ (deg)	90	90
<i>V</i> (Å <sup>3</sup> )	1509.6(2)	1583.8(6)
<i>Z</i>	4	4
calcd density (g cm <sup>-3</sup> )	1.524	1.452
abs coeff (mm <sup>-1</sup> )	0.774	0.738
<i>F</i> (000)	712	712
cryst size (mm)	0.357 × 0.147 × 0.043	0.406 × 0.303 × 0.222
$\theta$ range (deg); completeness (%)	2.15–27.00; 99.5	2.63–26.99; 99.9
limiting indices	–8 ≤ <i>h</i> ≤ +10, –15 ≤ <i>k</i> ≤ +16, –17 ≤ <i>l</i> ≤ +17	0 ≤ <i>h</i> ≤ +15, 0 ≤ <i>k</i> ≤ +17, –12 ≤ <i>l</i> ≤ +11
no. of rflns collected	8750	3450
no. of unique data	3283 ( <i>R</i> <sub>int</sub> = 0.0973)	3450 ( <i>R</i> <sub>int</sub> = 0.0894)
no. of data/restraints/ params	3283/2/228	3450/0/264
final <i>R</i> indices ( <i>I</i> > 2 $\sigma$ ( <i>I</i> )) <sup>a,b</sup>	<i>R</i> 1 = 0.0464, w <i>R</i> 2 = 0.0630	<i>R</i> 1 = 0.0514, w <i>R</i> 2 = 0.1423
<i>R</i> indices (all data) <sup>a,b</sup>	<i>R</i> 1 = 0.1293, w <i>R</i> 2 = 0.0796	<i>R</i> 1 = 0.1214, w <i>R</i> 2 = 0.2043
goodness of fit on <i>F</i> <sup>c</sup>	0.856	0.577
largest diff peak and hole (e Å <sup>-3</sup> )	0.286 and –0.363	0.509 and –0.433

<sup>a</sup> *R*1 =  $\sum|F_o| - F_c|/\sum|F_o|$ . <sup>b</sup> w*R*2 =  $\{\sum[w(F_o^2 - F_c^2)^2]/\sum[w(F_o^2)^2]\}^{1/2}$ .  
<sup>c</sup> GOF =  $\{\sum[w(F_o^2 - F_c^2)^2]/(n - p)\}^{1/2}$ .

**Conversion of 1 into 2 in Diethyl Ether.** **1** (1.5 g) was dissolved in 500 mL of degassed diethyl ether, the solution was then introduced in equal portions into eight glass tubes, and the tubes were sealed and let stand for different time

intervals at ambient temperature while avoiding sunlight. After respective time intervals, volatiles were removed in vacuo and the crude yellow solid was purified by column chromatography. Three fractions (**1**, **2**, and AECz) were obtained, quantified, and identified by <sup>1</sup>H NMR, respectively.

**Attempted Conversion of 2 into 1 in Solution.** Treatment of **2** was performed analogously to that of **1**. Even after the samples of **2** were maintained at ambient temperature for more than 60 h in solution (diethyl ether or THF), spectral evidence for the process of **2** → **1** was absent.

**Crystallography.** Single crystals of **1** and **2** suitable for X-ray diffraction were obtained by recrystallization from CH<sub>2</sub>-Cl<sub>2</sub>/hexane at –5 °C. X-ray data were collected on a Bruker Smart Apex CCD diffractometer and on a Rigaku AFC7R diffractometer, respectively. The structures were solved by direct methods using SHELXS97 and refined by the full-matrix least-squares method on all *F*<sup>2</sup> data using the program SHELXL97.<sup>16,17</sup> All non-hydrogen atoms were refined anisotropically. Hydrogen atoms were inserted in idealized positions and refined using a riding model. In the cell-packing graphs of **1** and **2** ordered *R* and *S* isomers in a ratio of 50/50 were observed in each complex. Further details are summarized in Table 2.

**Acknowledgment.** We thank the National Natural Science Foundation of China (Grant No. 20274011), the Development Project of Shanghai Priority Academic Discipline, and the Key Laboratory of Molecular Engineering of Polymers (Fudan University, Ministry of Education) for financial support.

**Supporting Information Available:** Tables of atomic coordinates, thermal parameters, and all bond distances and angles for **1** and **2**. This material is available free of charge via the Internet at <http://pubs.acs.org>.

OM0495527

(16) Sheldrick, G. M. SHELXS-97, Program for Crystal Structure Solution; University of Göttingen, Göttingen, Germany, 1997.

(17) Sheldrick, G. M. SHELXS-97, Program for Crystal Structure Refinement; University of Göttingen, Göttingen, Germany, 1997.